Proceedings of the Indian National Science Academy (2023) 89:869–883
https://doi.org/10.1007/s43538-023-00197-3

RESEARCH PAPER

RUSLE and AHP based soil erosion risk mapping for Jalpaiguri district of West Bengal, India

Jyotirmoy Biswas[1] · Biswajit Giri[1]

Received: 28 November 2022 / Accepted: 7 August 2023 / Published online: 12 September 2023

Abstract

Soil erosion has been identified as one of the serious environmental issues which reduces soil fertility by removing topsoil. An integrated method has been adopted in the present study to estimate average annual soil loss in Jalpaiguri district of Indian state of West Bengal by Revised Universal Soil Loss Equation (RUSLE) model and Analytic Hierarchy Process (AHP) method. The study also includes estimation of soil loss in different land use and land cover classes and different administrative blocks. RUSLE model estimates average annual soil loss in t ha^{-1} year^{-1} by calculating combined effects of rainfall erosivity, soil erodibility, slope length and steepness, land cover and conservation practices factors. Eight geo-environmental variables, i.e., rainfall erosivity, soil erodibility, slope, relative relief, drainage density, lineament density, land use/land cover and geomorphology has been incorporated in AHP method to estimate soil erosion. The models have been validated by Receiver Operating Characteristic curve. Area Under Curve value of both RUSLE model (0.91) and AHP method (0.82) gives satisfactory result. More than 25% area of northern hilly terrain and eastern alluvial plain of Jalpaiguri district are prone to severe and very severe soil erosion. Vegetation cover shows maximum percentage of areas in very severe soil erosion. Vegetation cover of Nagrakata block and agricultural lands of Dhupguri block are most vulnerable to soil loss due to sheet and rill erosion.

Keywords Rill erosion · Sheet erosion · Rainfall erosivity · Soil erodibility · Conservation practices

Introduction

Soil erosion is the continuous process of detachment and subsequent removal of topsoil by the physical forces of water and wind (Pal and Shit 2017). Removal of top soil reduces soil fertility (Chakrabortty et al. 2020). In recent times, soil erosion has been identified as one of the serious environmental issues which affects both agricultural and forested lands (Biswas 2012). Globally, almost 85% of land loss results from soil erosion processes (Angima et al. 2003). Tropical and semi-arid countries face the problem of sustainable agricultural productivity and poor water quality due to deterioration of the soil fertility (Bhat et al. 2017; Prasannakumar et al. 2012). Water induced soil erosion is the most significant degradation process, with global estimate of 11 million km^2 (Koirala et al. 2019) which accounts 56% of world's area (Tirkey et al. 2013). Rill and inter-rill erosion made up water induced soil erosion (Beskow et al. 2009). Rill erosion is the process of detachment and removal of top soil by small channels of concentrated water flow, whereas raindrops detaches and shallow overland flow transports top soil in inter-rill erosion (Demirci and Karaburun 2012). Inter-rill erosion is also known as sheet erosion (Mohammadi et al. 2018). Water induced soil erosion is a major problem in sub-humid and sub-arid regions of India which is accelerated by anthropogenic factors i.e., deforestation and unscientific agricultural practices (Pal and Shit 2017). Soil erosion affects more than 50% of land in India (Saha et al. 2018; Shit et al. 2015) which accounts for annual loss of 74 million tonnes of major nutrients (Rajbanshi and Bhattacharya 2020). Jain et al.(2001) has estimated that India experiences average annual soil loss rate of 16 t h^{-1} year^{-1}. It has been estimated that 1100 million hectares of land in India is affected by water induced soil erosion (Saha 2003) which

✉ Jyotirmoy Biswas
geographer.jyotirmoy@gmail.com

Biswajit Giri
biswajit_giri@yahoo.com

[1] Jadavpur University, Kolkata 700032, India

accounts for 56% of land affected by soil erosion (Biswas and Pani 2015).

There are a number of soil erosion models developed in recent decades. Mostly they are divided into physical, semi-empirical and empirical based models (Ghosh and Lepcha 2019). Universal Soil Loss Equation (USLE) (Wischmeier and Smith 1965), Modified Universal Soil Loss Equation (MUSLE) (Smith et al. 1984) and Revised Universal Soil Loss Equation (RUSLE) (Renard et al. 1991) are the most used empirical models. RUSLE model estimates average annual soil loss by sheet and rill erosion more accurately (Pan and Wen 2014) at reasonable costs by integration of Remote Sensing (RS) and Geographical Information System (GIS) techniques (Prasannakumar et al. 2011). Rainfall, soil, slope, land cover and conservation practice factors determine rate of soil erosion in RUSLE model (Bhattacharya et al. 2021). Several probabilistic and machine learning methods have been developed based on geo-environmental variables (Das et al. 2020) such as Artificial Neural Network (ANN), Analytic Hierarchy Process (AHP), Random Forest (RT), Weight of Evidence (WoE), Frequency Ratio (FR), Regression Tree (RT), etc. (Saha et al. 2022). AHP is a powerful decision-making method for estimation of soil erosion by placing different geo-environmental variables in a hierarchical structure (Thomas et al. 2018). The present study aims at finding average annual soil loss in Jalpaiguri district of Indian state of West Bengal using RUSLE model and AHP method. The study also aims at finding average annual soil loss in different land use and land cover (LULC) classes and administrative blocks of Jalpaiguri district.

Study area and database

Study area

Jalpaiguri is a northern district of Indian state of West Bengal. It shares international borders with Bhutan and Bangladesh in the north and south, respectively. Jalpaiguri district shares borders with Darjeeling district in the west, Kalimpong district in the north and Alipurduar and Coach Behar district on the east of West Bengal. Geographically, the district lies in between 26°15′47″N–26°59′34″N latitude and 88°23′2″E–89°7′30″E longitude. Jalpaiguri district covers 3,386.18 km^2 of geographical area. The district is divided into seven administrative blocks i.e., Dhupguri, Maynaguri, Rajganj, Jalpaiguri, Matiali, Mal and Nagrakata (See Fig. 1).

Jalpaiguri is a part of south-east Asian monsoon climate zone with average annual rainfall is 3360 mm. Average maximum temperature of 29 °C and average minimum temperature of 14 °C has been recorded. Northern hilly terrain, central tract of Bhaber and alluvial plain of Terai constitutes three physiographic units. Clayey loam, loam and sandy loam are the major soil types. Teesta, Jaldhaka,

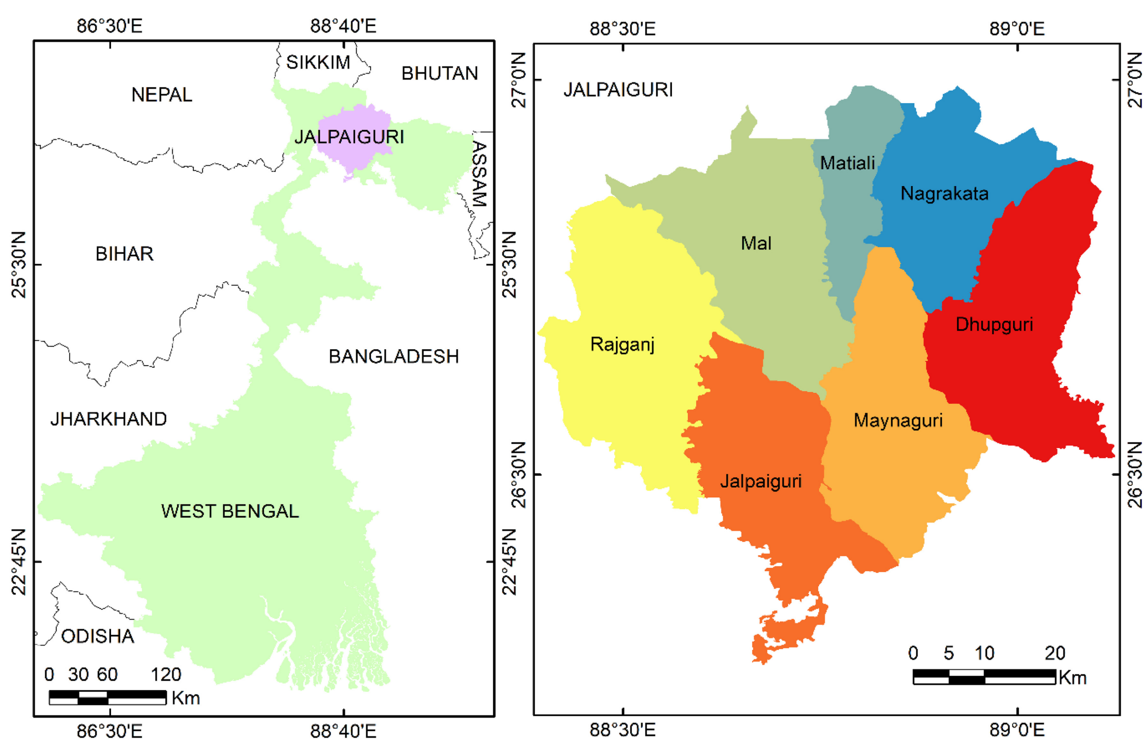

Fig. 1 Location map of the study area

Angrabhasa and Mahananda are the four major rivers of Jalpaiguri district. The district contains national protected areas like Gorumara National Park and Chapramari Wildlife Sanctuary. Majority of the people are associated with agricultural activities. Paddy is the principal crop, whereas tea is the most valuable crop (District Survey Report of Jalpaiguri District 2021).

Database

Village level shapefile of West Bengal, India has been downloaded from Socioeconomic Data and Applications Center (SEDAC) web portal for preparation of study area map. SEDAC is one of the Earth Observing System Data and Information System (EOSDIS) centers of United States National Aeronautics and Space Administration (NASA) (Linberger 1999). To prepare R factor map, daily rainfall data for 10 years (2011–2020) in milimeter (mm) has been downloaded from the web portal of Indian Meteorological Department (IMD), Pune. IMD provides rainfall data at 0.5 × 0.5 degree gridded resolution (Mitra et al. 2013) in NetCDF file. Digital Soil Map of the World (DSMW) in shapefile and data of different soil unit parameters have been downloaded from Food and Agriculture Organization (FAO) web portal of United Nations at a scale of 1:5,000,000 (FAO-Unesco 1974) to prepare K factor map. Cartosat-1 Digital Elevation Model (DEM) has been collected from Indian Space Research Organisation's (ISRO) Bhuvan geoportal to prepare slope, relative relief, drainage density and LS factor map. Two CartoDEM version-3 R1 scenes with 30 m spatial resolution (Yadav and Bhardwaj 2022) have been downloaded which covers the present study area. The two DEM scenes have been identified by the location of its south-west pixel's geometric centre which are 26°N 88°E and 26°N 89°E. Multispectral satellite images of Landsat 8 satellite have been collected from United States Geological Survey's (USGS) web portal. Operational Land Imager (OLI) sensor of Landsat 8 captures data in visible, panchromatic, near infrared (NIR) and shortwave infrared (SWIR) regions of electromagnetic spectrum (Acharya et al. 2015) which have been used in the present study. Except panchromatic band (15 m), all bands of OLI sensor are having 30 m spatial resolution (Knight and Kvaran 2014). Two cloud free images of 7th November 2020 having path no. 139 and row no. 41 and 42 have been used to calculate C and P factors. Geomorphology and lineament density map have been prepared from thematic services of ISRO's Bhuvan geoportal. All the data types along with their sources and purposes have been listed in Table 1.

Methodology

Rainfall erosivity (R) factor

R factor represents ability of raindrops to detach the soil particles based on volume and intensity of rainfall (Roy and Mitra 2022). It is the driving forces for rill and sheet erosion (Mahala 2018). Daily rainfall data for 10 years (2011–2020) has been collected from IMD, Pune. The present study area of Jalpaiguri district contains 10 grids of rainfall data in NetCDF file. Each grid has been identified by latitude and longitude of the geometric centre. Mean monthly and mean annual rainfall has been determined for each year and R factor values for each year has been calculated using the following Eq. 1 of Wischmeier and Smith (1978) and Arnoldus (1980).

$$R = \sum_{i=1}^{12} 1.735 \times 10^{\left[1.5 \times log_{10}\left(\frac{P_i^2}{P}\right) - 0.08188\right]}, \tag{1}$$

where P_i is average monthly rainfall in mm and P is average annual rainfall in mm (Markose and Jayappa 2016). Kriging interpolation (Eq. 2) method has been employed taking 10 years average R factor values to get the desired R factor map (Fig. 2a).

$$Z_0 = \sum_{\mathbf{i=1}}^{n} \lambda_i Z_i \tag{2}$$

(Sarkar et al. 2021) where, Z_0 is the estimated value at unknown location, Z_i is known values, λ_i is weightage coefficient and n are the number of neighbourhoods searching data points.

Table 1 List of data types with their sources and purposes

S. no.	Data type	Source	Purpose(s)
1	Village level shapefile	https://sedac.ciesin.columbia.edu	Study area map
2	Rainfall	https://www.imdpune.gov.in	R factor map
3	Soil	https://data.apps.fao.org/map/catalog	K factor map
4	DEM	https://bhuvan-app3.nrsc.gov.in	Slope, drainage density, relative relief and LS factor map
5	Satellite image	https://earthexplorer.usgs.gov	C and P factor map
6	Geomorphology	https://bhuvan-app1.nrsc.gov.in	Geomorphology map
7	Lineament	https://bhuvan-app1.nrsc.gov.in	Lineament density map

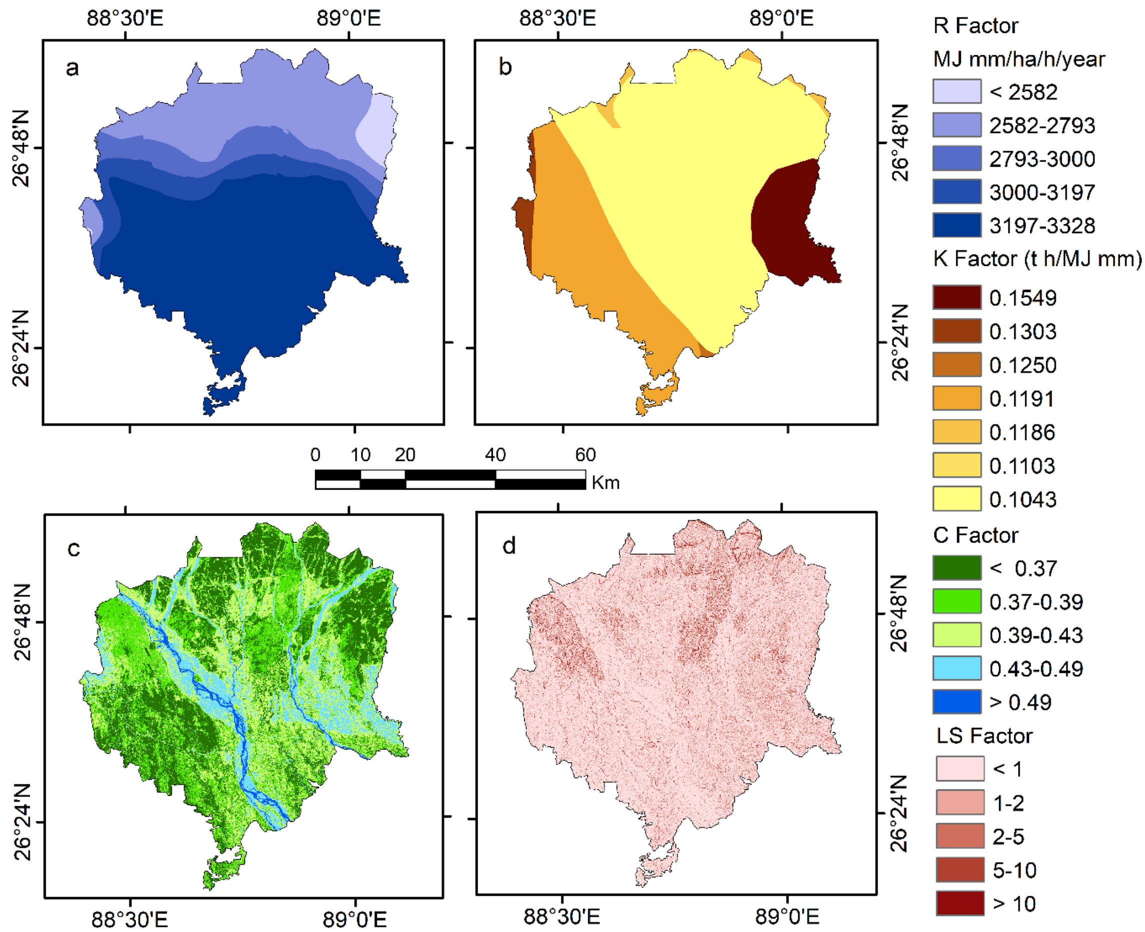

Fig. 2 **a** R, **b** K, **c** C, **d** LS factor map of Jalpaiguri district

Soil erodibility (K) factor

K factor reflects the susceptibility of soil particles removal by water induced soil erosion (Kulimushi et al. 2021). It is the rate of soil loss per unit R factor index for a specific soil unit (Belasri and Lakhouili 2016). Taking soil textures into consideration (Ganasri and Ramesh 2016), K factor map has been created using following Eq. 3 of Williams (1995).

$$K = F_{csand} \times F_{cl-si} \times F_{org} \times F_{hisand}, \tag{3}$$

where, F_{csand} indicates lower K factors for high coarser sand content, F_{cl-si} reduces K factors for high clay and silt ratios, F_{org} reflects low K factors for high organic carbon content and F_{hisand} reduces K factors for very high sand content (Wawer et al. 2005).

$$F_{csand} = 0.2 + 0.3 \times e^{\left[-0.256 \times m_s \times \left(1 - \frac{m_{silt}}{100}\right)\right]},$$

$$F_{cl-si} = \left(\frac{m_{silt}}{m_c + m_{silt}}\right)^{0.3},$$

$$F_{org} = 1 - \frac{0.25 \times orgC}{orgC + e^{(3.72 - 2.95 \times orgC)}},$$

$$F_{hisand} = 1 - \frac{0.7 \times \left(1 - \frac{m_{silt}}{100}\right)}{\left(1 - \frac{m_{silt}}{100}\right) + e^{\left[-5.51 + 22.9 \times \left(1 - \frac{m_s}{100}\right)\right]}},$$

where m_s is % of sand, m_{silt} is % of silt, m_c is % of clay and $orgC$ is % of organic carbon content in top soil.

The vector soil map for the study area has been extracted from the DSMW in ArcGIS 10.8. The values of F_{csand}, F_{cl-si}, F_{org} and F_{hisand} have been calculated for respective soil unit exists in the study area in MS Excel taking the topsoil data of m_s, m_{silt}, m_c and $orgC$ (Table 2). K factor values have been calculated subsequently for each soil units present in the

Table 2 K factor values of different soil units

Soil unit	m_s	m_{silt}	m_c	orgC	F_{csand}	F_{cl-si}	F_{orgC}	F_{hisand}	K factor
Bd	32.7	30.3	37.1	3.28	0.2010	0.7867	0.7502	1.0000	0.1186
Be	36.4	37.2	26.4	1.07	0.2010	0.8514	0.9054	0.9999	0.1549
Bh	55.2	21	23.8	3.86	0.2000	0.7967	0.7500	0.9973	0.1192
Ge	42.8	20.4	36.8	1.3	0.2001	0.7340	0.8517	0.9998	0.1250
Je	70.8	12.8	16.5	1.15	0.2000	0.7800	0.8867	0.9421	0.1303
Nd	38.9	17.6	43.6	1.57	0.2001	0.6881	0.8010	0.9999	0.1103
Rd	82.1	6.7	11.3	0.27	0.2000	0.7434	0.9964	0.7037	0.1043

study area and attached to the attribute table of extracted soil map. The projected vector soil map in WGS 1984 UTM Zone 45 N has been converted to raster using K factor value field with 30 m cell size to get the desired K factor map (Fig. 2b).

Slope (S) and slope length and steepness (LS) factor

L factor gives the impact of slope length while S factor accounts for the effect of slope steepness on the rate of water induced soil erosion (Negese et al. 2021). The LS factor is dimensionless (Mahala 2018), having values greater than equal to zero. Cartosat DEM with 30 m spatial resolution has been used for computation of the slope and LS factor using the following Eq. 4 of Moore and Burch (1986).

$$LS = \left[fa \times \frac{s}{22.13}\right]^{0.4} \times \left[\frac{\sin\theta}{0.0896}\right]^{1.3}, \quad (4)$$

where fa is flow accumulation, s is cell size and θ is slope in radian. Slope raster in degree has been created from the projected DEM in WGS 1984 UTM Zone 45 N of the study area. Slope in degree has been converted to slope in radian by multiplying π/180 in raster calculator of ArcGIS 10.8 (Fig. 3a). The depression less DEM has been used to create flow direction and flow accumulation raster. Equation 4 has been employed in raster calculator to get the desired LS factor map (Fig. 2d).

Relative relief (RR) and drainage density (DD)

Relative Relief is defined as the difference of the maximum and minimum elevation, i.e., elevation range. 100×100 fishnet has been prepared in ArcGIS and geometric centre of each fishnet has been assigned with relative relief values using range statistics type of *zonal statistics as table* tool. Kriging interpolation (Eq. 2) has been used to get the desired relative relief map (Fig. 3b).

Drainage Density is defined as the ratio of length and area of the drainage. It is expressed in mm^{-2}. It has been prepared from the flow accumulation raster of Cartosat DEM by converting it to stream raster, stream order and then stream vector. *Line density* from spatial analyst tools in ArcGIS environment has been employed to get the desired drainage density map (Fig. 3c).

Geomorphology (G) and lineament density (LD)

Both geomorphology and lineament features have been extracted from the thematic services of ISRO's Bhuvan geoportal. Web Map Service (WMS) layer of geomorphology and lineament has been processed in QGIS. *Line density* tool within the ArcGIS environment has been utilized to generate lineament density map.

Supervised classification and accuracy assessment

Landsat 8 multispectral images of the study area have been used to do a supervised image classification in Erdas Imagine 2018. Five major LULC classes i.e., vegetation, water body, agriculture, bare land and built-up areas have been identified. More than 50 training sets for each LULC classes have been taken for signature generation. Parallelepiped non-parametric classifier algorithm has been employed to carry out supervised image classification. Maximum likelihood parametric classifier algorithm has been applied for unclassified pixels of non-parametric rule. The maximum likelihood classification algorithm applies probability theory for classification by determining class centres and variability in raster values, whereas parallelepiped classifier depends on the selection of lowest and highest values of each class (Bhatta 2020).

Accuracy assessment in image classification is a feedback system for checking and evaluating results (Bhatta 2020). Equalized stratified random sampling technique has been adopted to get 10 random points for each of the five LULC classes. Confusion matrix has been prepared by taking classification results in rows and ground truth reference from Google Earth in columns for each sample point. Overall accuracy and kappa statistic of classification has been calculated from the confusion matrix (Table 3) using following Eqs. 5 and 6 respectively.

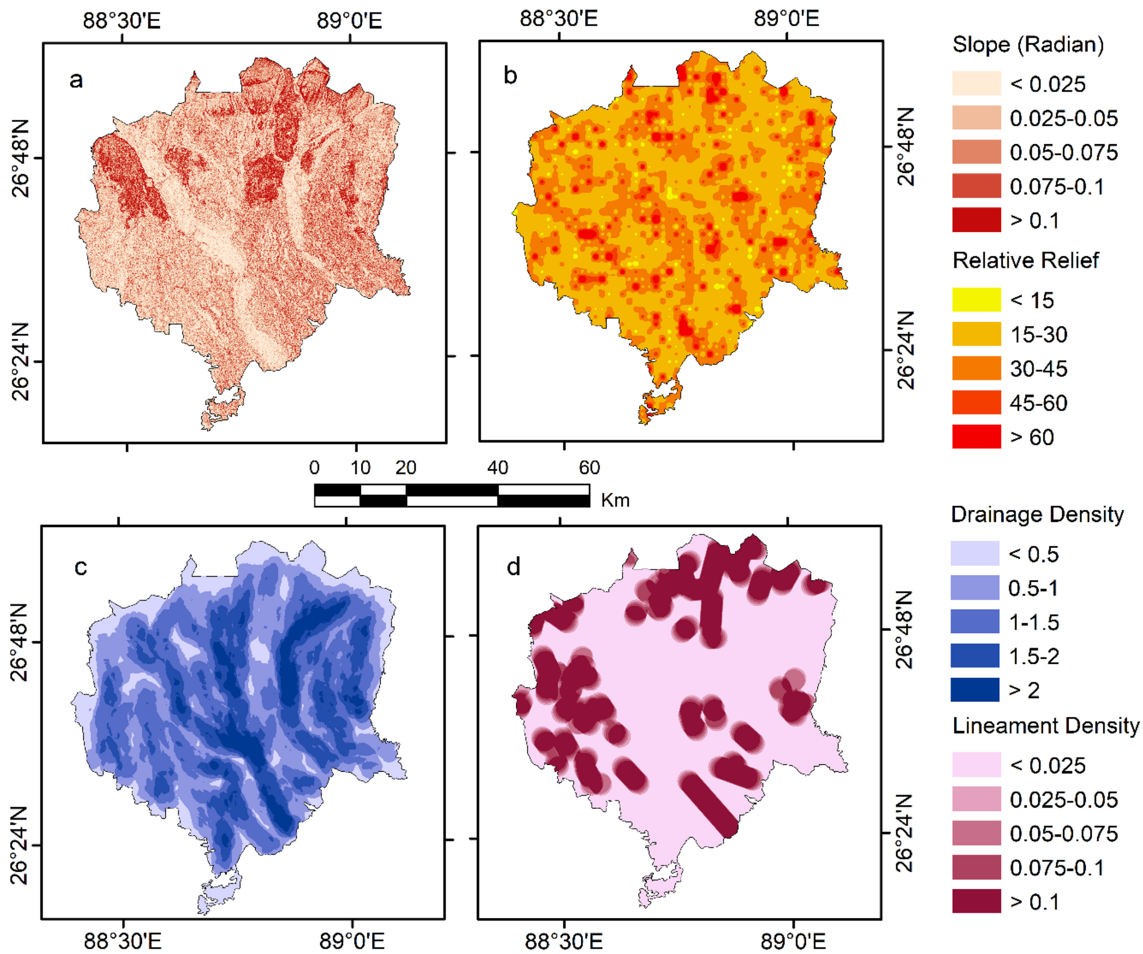

Fig. 3 **a** Slope, **b** relative relief, **c** drainage density, **d** lineament density map of Jalpaiguri district

Table 3 Overall accuracy and kappa statistic of supervised classification

LULC classes	Vegetation	Water body	Agriculture	Bare land	Built-up	Total	User's accuracy (%)
Vegetation	10	0	0	0	0	10	100
Water body	0	8	1	1	0	10	80
Agriculture	0	0	10	0	0	10	100
Bare land	0	0	1	9	0	10	90
Built-up	0	0	1	0	9	10	90
Total	10	8	13	10	9	50	
Producer's accuracy	100%	100%	77%	90%	100%		
Overall accuracy		92%					
Kappa statistic		0.9					

$$\omega = \frac{\sum_{i=1}^{n} e_{ii}}{N} \times 100, \tag{5}$$

where ω is overall accuracy, e_{ii} is element of i^{th} row and i^{th} column, n is total number of classes and N is total number of samples.

$$\kappa = \frac{\left(N \times \sum_{i=1}^{n} e_{ii}\right) - Chance\ agreement}{N^2 - Chance\ agreement}, \tag{6}$$

where κ is kappa statistic and *Chance agreement* = *ΣProduct of row total and column total for each class*.

Land cover (C) factor

Soil erosion is greatly influenced by amount and type of land cover because vegetation cover prevents direct impact of rainfall on soil (Das et al. 2018). C factor is defined as the ratio of soil loss from agricultural cropped land and clean tilled continuous fallow under same slope and rainfall condition (Pandey et al. 2007). Normalized Difference Vegetation Index (NDVI) and C factor are correlating with a positive relationship (Benavidez et al. 2018). C factor value ranges between '0' and '1', where '0' represents low vulnerability and '1' represents high vulnerability (Mahala 2018). The C factor map has been created using the following Eq. 7 proposed by Durigon et al. (2014).

$$C = \frac{1 - NDVI}{2}, \tag{7}$$

where

$$NDVI = \frac{NIR - \mathrm{Re}d}{NIR + \mathrm{Re}d}$$

The NDVI map has been prepared using Red and NIR bands of the LANDSAT 8 multispectral images of the study area in raster calculator of ArcGIS 10.8. Desired C factor map (Fig. 2c) has been created using the Eq. 7 in raster calculator.

Conservation practices (P) factor

P factor is considered as the effects of erosion preventive practices such as terrace farming, strip cropping, contour ploughing, etc. to reduce soil erosion (Ashiagbor et al. 2013). P factor values can be identified from the LULC types (Naqvi et al. 2013). P factor value ranges between '0' and '1' (Tanyaş et al. 2015), where '0' indicates highest effectiveness of conservation practices and '1' indicates no conservation practices implemented (Santra and Mitra 2020).

P factor values have been collected from the literature (Table 4) due to lack of data on conservation practices in the study area. P factor values has been added to the attribute table of the LULC raster and a new raster of P factor has been created using the P factor value field using *Lookup* tool of ArcGIS 10.8 (Fig. 4b).

RUSLE model

RUSLE model is a straightforward and empirically based model that has the ability to predict long term average annual soil loss by sheet and rill erosion using data on rainfall pattern, soil type, topography, crop system and management practices (Teng et al. 2018). The average annual soil loss (A) in RUSLE model has been described by the following Eq. 8 of Renard et al. (1991).

$$A = R \times K \times LS \times C \times P \tag{8}$$

All the five RUSLE factor rasters have been multiplied in in raster calculator in ArcGIS to get the average annual soil loss map.

AHP method

AHP is a multi-criteria decision-making method based on different hierarchical geo-environmental variables (Das et al. 2020). In this study, the variables considered are rainfall erosivity, soil erodibility, slope, relative relief, drainage density, lineament density, geomorphology and land use/land cover. The semi-qualitative AHP method employed here utilizes a matrix based on pair-wise comparisons to assess the contribution of various variables (Pradeep et al. 2015). In AHP method, variables are compared against each other to determine their relative preferences, which are then quantified using numeric values. The matrix elements (a_{ij}) can be described by following Eq. 9 of Saaty (1980):

$$a_{ij} = \frac{w_i}{w_j} = \frac{weight\ of\ \mathrm{varibale}\ i}{weight\ of\ \mathrm{varibale}\ j} \tag{9}$$

Table 4 P factor values for different LULC classes

S. no.	LULC Classes	P factor	Sources
1	Vegetation	1	Das et al. (2018), Prasannakumar et al. (2011), Tirkey et al. (2013)
2	Water body	1	Mahala (2018), Naqvi et al. (2013), Tirkey et al. (2013)
3	Agriculture	0.28	Mahala (2018), Pandey et al. (2007), Saha et al. (2018)
4	Bare land	1	Bhat et al. (2017), Das et al. (2018), Nasir and Selvakumar (2018)
5	Built-up	0	Bhat et al. (2017), Nasir and Selvakumar (2018), Rahaman et al. (2015)

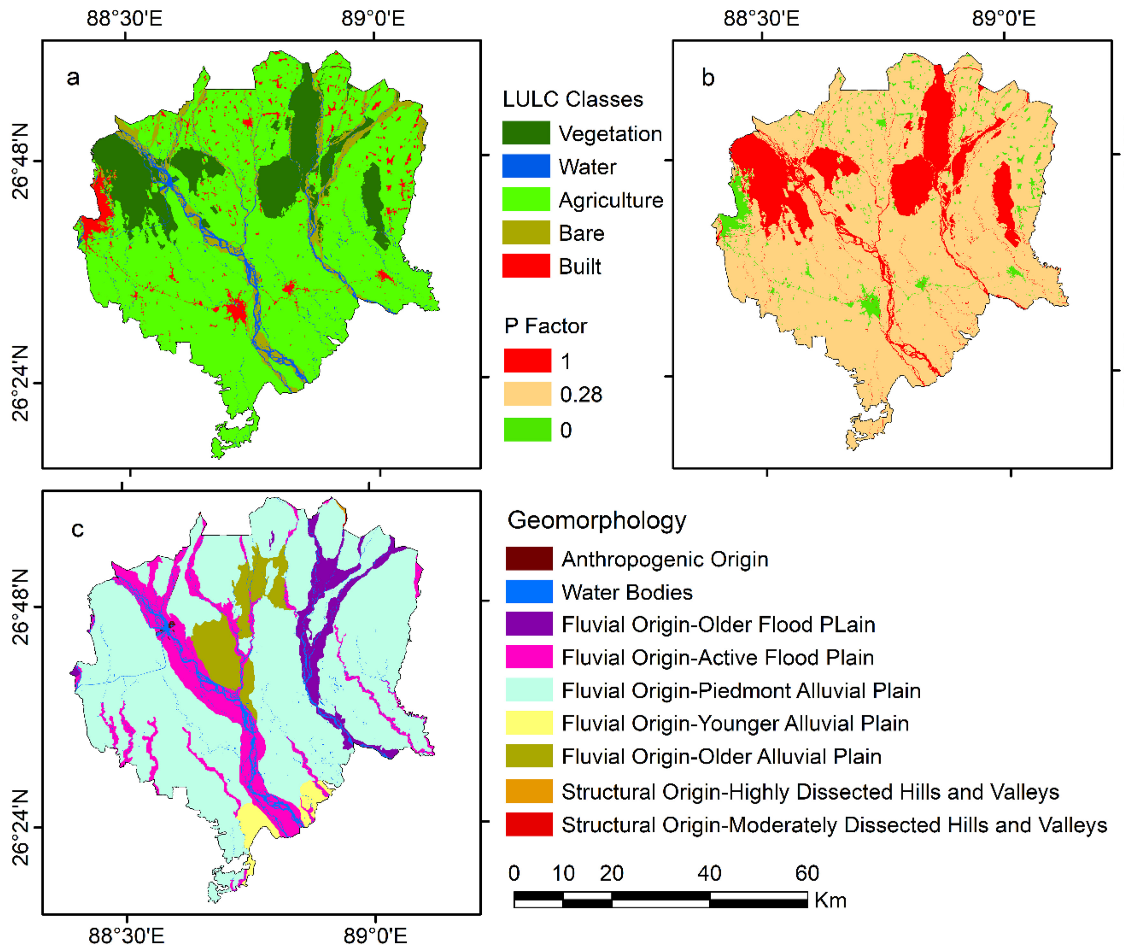

Fig. 4 **a** LULC, **b** P factor, **c** geomorphology map of Jalpaiguri district

The weights assigned to the variables can range from 1 to 9, where 1 indicates equal importance and 9 indicates absolute importance (Thomas et al. 2018). The eigenvector method has been employed to determine weight of each variable (Das et al. 2020). The primary eigenvalues have been computed by summing each column in the pairwise comparison matrix. Subsequently, the values in each cell have been divided by the column sum for normalization. The average of each row elements of normalized matrix gives the eigenvalue of each variable. To access the degree of consistency of the pairwise matrix, the Consistency Index (CI) and Consistency Ratio (CR) has been computed (Mihi et al. 2020) using Eqs. 10 and 11:

$$CI = \frac{\lambda_{\max} - n}{n - 1} \tag{10}$$

$$CR = \frac{CI}{RI} \tag{11}$$

where λ_{max} is the principal eigenvalue and $\boldsymbol{n}$ is the number of variables. ***RI*** is the random index defined by Saaty (1980) for different value of $\boldsymbol{n}$ (Table 5). CR < 0.1 indicates an acceptable level for the variables in the analysis.

Finally weighted overlay analysis has been done in ArcGIS to prepare Soil Erosion Risk Index (SERI) by the following Eq. 12:

$$SERI = \sum_{i=1}^{n} E_i \times V_i \tag{12}$$

where, E_i is the eigenvalue of different variables V_i.

Table 5 RI values of Saaty depending on number of variables

n	1	2	3	4	5	6	7	8	9	10
RI	0	0	0.58	0.9	1.12	1.24	1.32	1.41	1.45	1.49

Results and discussions

Rainfall erosivity (R) factor

R factor of the Jalpaiguri district ranges from 2,254 MJ mm ha^{-1} h^{-1} $year^{-1}$ to 3,328 MJ mm ha^{-1} h^{-1} $year^{-1}$ (Fig. 2a). The R factor map has been classified into five erosivity zones i.e., lowest (2254–2582 MJ mm ha^{-1} h^{-1} $year^{-1}$), low (2582–2793 MJ mm ha^{-1} h^{-1} $year^{-1}$), moderate (2793–3000 MJ mm ha^{-1} h^{-1} $year^{-1}$), high (3000–3197 MJ mm ha^{-1} h^{-1} $year^{-1}$) and highest (3197–3328 MJ mm ha^{-1} h^{-1} $year^{-1}$). Southern part of the study area shows highest R factor values which covers more than 50% of the area. The northern part shows low rainfall erosivity, whereas a small patch of land in north-eastern part shows lowest value. Moderate and high R factor values can be seen in the central part of the study area. The general trend of R factor shows rainfall erosivity increases from north to southern direction of the Jalpaiguri district.

Soil erodibility (K) factor

K factor of Jalpaiguri district varies from 0.1043 to 0.1549 t h MJ^{-1} mm^{-1} (Fig. 2b). The K factor map has been classified by unique values of different soil units present in the study area. Dystric Regosils (Rd) soil unit shows lowest (0.1043 t h MJ^{-1} mm^{-1}) K factor value which covers most of the study area. Eutric Cambisols (Be) soil unit in south-eastern part shows highest (0.1549 t h MJ^{-1} mm^{-1}) K factor value. Humic Cambisols (Bh) in western part and narrow stipe of Eutric Fluvisols (Je) in west shows moderate (0.1192 t h MJ^{-1} mm^{-1}) and high (0.1303 t h MJ^{-1} mm^{-1}) K factor values respectively. Dystric Cambisols (Bd), Eutric Gleysols (Ge) and Dystric Nitosols (Nd) soils are present in few smaller patches.

Relative relief (RR), drainage density (DD) and lineament density (LD)

Relative relief (Fig. 3b), drainage density (Fig. 3c) and lineament density (Fig. 3d) map has been classified into five classes. Majority of the district has been categorized as very low (<15) and low (15–30) in terms of relative relief. However, significant patches of high (45–60) and very high (>60) relative relief is scattered throughout the study area. High (1.5–2 mm^{-2}) and very high (>1.5 mm^{-2}) drainage density can be witnessed throughout the district due to presence of major rivers and its tributaries. Northern hilly terrain and western and south–eastern alluvial plain shows high (0.075–0.1) and very high (>0.1) lineament density. Majority portion of the area is categorized as very low (<0.025) lineament density.

Slope (S) and slope length and steepness (LS) factor

The slope ranges from 0 to 0.8 rad (Fig. 3a), whereas unitless LS factor of Jalpaiguri district ranges from 0 to 632 (Fig. 2d). Mean and standard deviation of LS factor have been found to be 0.73 and 5.06 respectively. Significant portion of the study area can be classified as high (0.075–0.1 rad) slope, whereas majority portion is classified as very low (<1) LS factor value. Few patches of high (5–10) and very high (>10) LS factor can be seen in north and northwestern part due to presence of hilly terrain. Low (1–2) and moderate (2–5) values are scattered over the whole study area. General trend of slope and LS factor is decreasing from north to southern direction.

Accuracy assessment and LULC

The supervised image classification of Jalpaiguri district has shown very high accuracy (Table 3). User's accuracy for vegetation and agricultural lands and producer's accuracy for vegetation, water body and built-up areas shows 100% accuracy. The overall accuracy and kappa statistic have been found to be 92% and 0.9 respectively.

The people of Jalpaiguri district are mostly engaged with agricultural activities which is evident from the fact that most of study area (71.83%) is covered by agricultural land (Fig. 4a; Table 6). Tea and paddy are the principal crops of northern hilly terrain and southern alluvial plain of Terai region. Significant amount of land (14.84%) in northern hilly terrain are covered by forest, whereas Bhaber and Terai regions are devoid of forest cover. Rivers, canal, ponds and wetlands contribute 3.21% of water bodies in the district. 3.77% of lands constitutes built-up areas. Rural and urban settlement, industrial areas and major highways constitutes built-up areas. Bare lands (6.35%) are mostly sand bars along the rivers.

Table 6 Percentage of area in each LULC classes

S. no.	LULC classes	Area (km^2)	Area (%)
1	Vegetation	506.8919983	14.84
2	Water body	109.6060028	3.21
3	Agriculture	2452.820068	71.83
4	Bare land	216.970993	6.35
5	Built-up	128.6609955	3.77

Land cover (C) factor

The unitless land cover factor ranges from 0.25 to 0.56 (Fig. 2c). The five C factor classes almost coincide with the LULC classes. The highest (0.49–0.56) and high (0.43–0.49) C factor values almost coincide with water bodies and bare lands which are more prone to erosion. Built-up areas also show high land cover factor. Very low (0.25–0.37), low (0.37–0.39) and moderate (0.39–0.43) C factor values represents forest and agricultural lands.

Conservation practices (P) factor

P factor map has been classified by its three unique values (Fig. 4b). Forest, bare land and water bodies have been assigned the highest P factor value of '1' due to no conservation practices. Least P factor value of '0' has been assigned to built-up areas. Since built-up areas covers the topsoil, it is least prone to erosion. Agricultural lands are prone to erosion based on different conservation practices have been applied. P factor value of 0.28 has been assigned to agricultural lands due to lack of conservation practices data of Jalpaiguri district.

Geomorphology

Geomorphology of Jalpaiguri district comprises of fluvial origin, structural origin, anthropogenic origin and water bodies. Small patches of both highly and moderately dissected hills and valleys of structural origin can be seen at extreme north of the district. Majority of the study area is of fluvial origin. Among fluvial origin, alluvial plain is predominated. However, significant portion of land is flood plain. Piedmont alluvial plain is the most dominant geomorphology. Younger alluvial plain can be seen at extreme south, whereas older alluvial plain is in north-central portion. Area around Teesta river constitutes active flood plain, whereas area around Jaldhaka river is categorized as older flood plain.

Soil loss (A) estimation by RUSLE model

Soil loss of Jalpaiguri district have been classified into six erosion classes as recommended by Singh et al. (1992) and applied by Pandey et al. (2007) for Indian conditions (Fig. 5). Slight (< 5 t ha^{-1} $year^{-1}$), moderate (5–10 t ha^{-1} $year^{-1}$), high (10–20 t ha^{-1} $year^{-1}$), very high (20–40 t ha^{-1} $year^{-1}$), severe (40–80 t ha^{-1} $year^{-1}$) and very severe (> 80 t ha^{-1} $year^{-1}$) are the six erosion classes. Table 7 Shows percentage of area in different erosion classes. Most of area (50.18%) falls under slight erosion potential zone. Many patches of severe and very severe soil erosion areas can be seen in eastern, northern and north-western part of the district. More than 25% of the areas are affected by severe and very severe soil erosion. Moderate, high and very high soil erosion potential zones are scattered over the whole study area which contributes 4.95%, 8.39% and 10.88% of areas respectively.

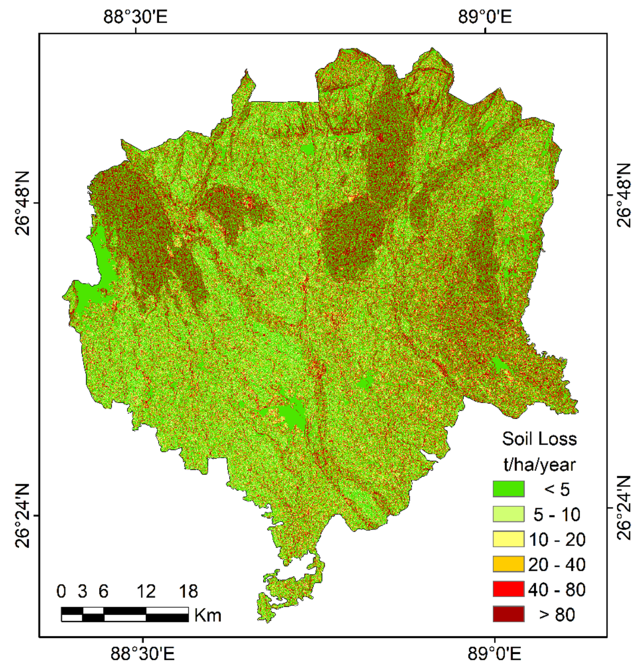

Fig. 5 RUSLE based soil loss map of Jalpaiguri district

Table 7 Percentage of soil loss in different erosion classes

S.no.	Soil loss (t ha^{-1} $year^{-1}$)	Erosion classes	Area (km^2)	Area (%)
1	< 5	Slight	1706.77	50.18
2	5–10	Moderate	168.51	4.95
3	10–20	High	285.37	10.88
4	20–40	Very high	370.02	9.63
5	40–80	Severe	327.52	9.63
6	> 80	Very severe	543.37	15.97

Soil erosion risk index (SERI) by AHP method

In decreasing order of weights, the geo-environmental variables are prioritized as follows: rainfall erosivity with the highest weight of 9, followed by slope (8), land use and land cover (6), relative relief (4), soil erodibility (3), geomorphology (3), lineament density (2), and drainage density (1) (Das et al. 2020; Mihi et al. 2020; Pradeep et al. 2015; Prakash et al., 2022; Saha et al. 2022). Pairwise comparison matrix has been presented in Table 8. The higher eigenvalue of 0.25 and 0.22 suggests rainfall and slope variable

Table 8 Pairwise comparison matrix and eigenvalue

	R	S	LULC	RR	G	K	LD	DD	Eigenvalue
R	1	1.125	1.5	2.25	3	3	4.5	9	0.25
S	0.889	1	1.333	2	2.667	2.667	4	8	0.22
LULC	0.667	0.75	1	1.5	2	2	3	6	0.17
RR	0.444	0.5	0.667	1	1.333	1.333	2	4	0.11
G	0.333	0.375	0.5	0.75	1	1	1.5	3	0.08
K	0.333	0.375	0.5	0.75	1	1	1.5	3	0.08
LD	0.222	0.25	0.333	0.5	0.667	0.667	1	2	0.06
DD	0.111	0.125	0.167	0.25	0.333	0.333	0.5	1	0.03
λ_{max} = 8.07975			CI = 0.01139286				CR = 0.00808004		

holds a relatively higher importance in the analysis, respectively. On the contrary, the eigenvalue of 0.03 and 0.06 for drainage density and lineament density are relatively less important in the analysis, respectively. A consistency value of 0.008, which is less than the threshold of 0.1, suggests that the weights assigned to the individual variables are consistent.

Similar to the classification scheme used in the RUSLE model, the Soil Erosion Risk Index (SERI) map generated through the Analytic Hierarchy Process (AHP) method has also been classified into six distinct classes (Fig. 6). These classes are categorized as slight, moderate, high, very high, severe, and very severe. In the Teesta floodplain and western alluvial plain, the majority of the area is categorized as slight to moderate erosion prone. This suggests a relatively lower risk of soil erosion in these regions compared to other areas. However, in contrast, the northern hilly terrain and eastern alluvial plains exhibit a significant portion of the area classified as severe to very severe erosion prone. This indicates a high vulnerability to soil erosion in these regions, emphasizing the need for targeted erosion control and conservation measures to mitigate the potential negative impacts on land productivity and environmental stability.

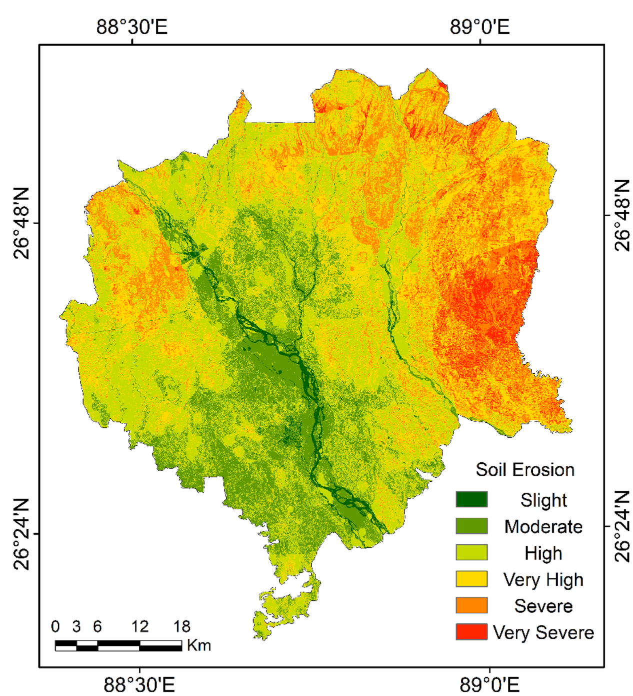

Fig. 6 AHP based soil erosion risk index map of Jalpaiguri district

Model validation by ROC curve

The validation of soil erosion models is widely recognized as one of the most crucial for accuracy and reliability of the models' predictions and ensuring their applicability in real-world scenarios (Gayen et al. 2019). In order to validate RUSLE model and AHP method, a total of 130 locations were randomly selected. The selected sites have been randomly classified as training (70%) and testing (30%) datasets in Python. These locations were then thoroughly examined using high-resolution imagery from Google Earth Pro software, covering various time scales. By utilizing the rich visual information provided by Google Earth Pro, a more comprehensive understanding of soil erosion dynamics and validation of the risk map has been achieved. Receiver Operating Characteristic (ROC) curves are frequently used to compare existing soil erosion locations in validation datasets with the aid of a soil erosion map (Ghosh and Maiti 2021). These curves provide a graphical representation of the model's performance by plotting the true positive rate (sensitivity) against the false positive rate (1-specificity) at various threshold values. By analysing the ROC curve, the model's accuracy, discrimination power, and overall performance in identifying soil erosion locations can be evaluated.

Area Under Curve (AUC) value is a commonly used metric to assess the performance models, particularly in the context of ROC curves (Bag et al. 2022). AUC value above 0.8 is considered as the excellent accuracy of the

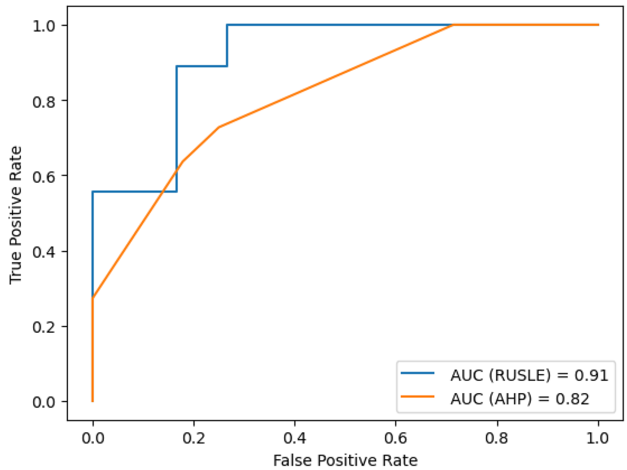

Fig. 7 ROC curve for RUSLE model and AHP method

model. In the present context, both the RUSLE model and the AHP method exhibit excellent accuracy, with AUC values of 0.91 and 0.82, respectively (Fig. 7). However, considering the higher AUC value of 0.91, the RUSLE model is deemed more appropriate compared to the AHP method. This suggests that the RUSLE model demonstrates a stronger predictive capability in assessing soil erosion risk in the given context.

Soil loss in LULC classes

Nearly 42% area of vegetation cover of Jalpaiguri district are potential zones of very severe soil erosion (Fig. 8). LS factor is the most responsible factor for higher rate of soil loss from the vegetation covers due to presence all forested areas in northern hilly terrain which have higher slope compared to rest of the district. More than 20% of agricultural lands are vulnerable to severe and very severe soil erosion. Loss of top fertile soil from the agricultural lands at higher rate is a great concern due to the fact that agriculture is the most common economic activity of the district. It shall be also responsible for lower yield per unit area of agricultural lands. Nearly 30% and 26% areas of water bodies and bare lands are prone to very severe soil erosion respectively. Erosion in the water bodies and bare lands signifies sediment transportation from the major rivers. Built-up areas do not show any erosion due to highest conservation practices factor.

Soil loss in administrative blocks

Nagrakata block is most vulnerable to soil erosion with 26.63% of area in very severe erosion category (Fig. 9). Presence of more vegetation cover in Nagrakata block accounts for higher soil loss. Both Matiali and Dhupguri blocks also shows nearly 20% area are prone to very severe soil erosion. Both vegetation cover and agricultural lands of

Fig. 8 Percentage of severe and very severe soil erosion in LULC classes

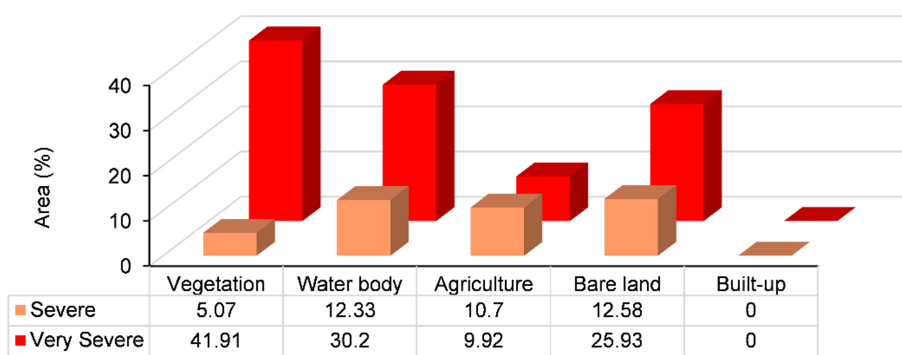

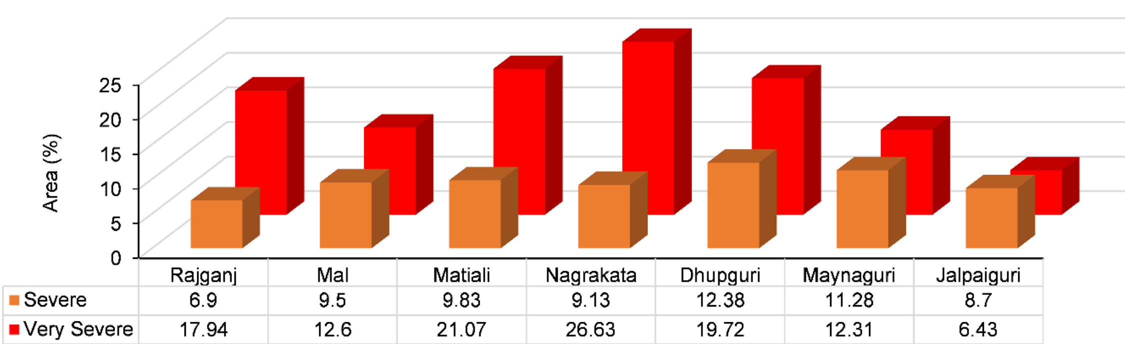

Fig. 9 Percentage of severe and very severe soil erosion in administrative blocks

Matiali block accounts for high soil loss. Agricultural lands contribute most of the areas of very severe soil erosion in Dhupguri block. Nearly 18% area of Rajganj block are prone very severe soil erosion which is also due to the presence of significant amount of vegetation cover. Maynaguri block also shows more than 10% area under very severe erosion category. Jalpaiguri block is the least vulnerable to soil erosion compared to other blocks of the district.

Conclusion

Soil erosion is a very serious issue for hilly region and its surrounding valley areas. Present study area of Jalpaiguri district faces this serious issue and the assessment of soil loss is indispensable for sustainable development. Sheet and rill erosion by water are common accumulators for soil vulnerability in this area. The erosion of soil is very low in maximum area but it may arise at a disquieting rate originating severe to very severe loss of top soil. Quantitative estimation of soil loss by water erosion in the study area has been accomplished by RUSLE model and AHP method with the aid of RS and GIS. The validation using ROC curves indicates that both the RUSLE and AHP models exhibit excellent accuracy in predicting soil erosion. However, the RUSLE model outperforms the AHP model with a higher AUC value of 0.91 compared to 0.82, indicating its superior capability in soil erosion prediction. According to the RUSLE model, more than 25% of the area in Jalpaiguri district is classified as prone to severe to very severe soil erosion. Northern hilly terrain and eastern alluvial plain are at more risk of soil erosion. Among the LULC classes, vegetation covers are found to experience higher soil loss. Sloping topography and unsuitable land use practices, such as improper agriculture and deforestation are the main causes of erosion in these regions. Specifically, in the Nagrakata block, the vegetation covers are particularly vulnerable to soil erosion. Additionally, agricultural lands in the Dhupguri block are also identified as highly erosion prone. Intensive farming practices and lack of conservation measures leave agricultural lands of these regions vulnerable to erosion. These findings emphasize the importance of implementing erosion control measures and land management practices in these areas to protect the vegetation covers and agricultural lands from soil erosion and maintain their productivity.

Supplementary Information The online version contains supplementary material available at https://doi.org/10.1007/s43538-023-00197-3.

Acknowledgements We would like to acknowledge the efforts of Suman Ghosh, Mala Ghosh, Baidyanath Hazra, Sanjay Sarkar, Debolina Baneerjee, Avijit Banerjee and Archana Saha for the collection of data and report writing.

Declarations

Conflict of interest There are no competing interests neither any conflict of interest and the work has completely done on secondary data. All data generated or analysed during this study are included in this manuscript (and its supplementary information files).

References

Angima, S.D., Stott, D.E., O'Neill, M.K., Ong, C.K., Weesies, G.A.: Soil erosion prediction using RUSLE for central kenyan highland conditions. Agric. Ecosyst. Environ. **97**(1–3), 295–308 (2003). https://doi.org/10.1016/S0167-8809(03)00011-2

Arnoldus, H.M.J.: An approximation of the rainfall factor in the universal soil loss equation. In: De Boodt, M., Gabriels, D. (eds.) Assessment of erosion. Wiley, Hoboken (1980)

Ashiagbor, G., Forkuo, E.K., Laari, P., Aabeyir, R.: Modeling soil erosion using RUSLE and GIS tools. Int. J. Remote Sens. Geosci. (IJRSG) **2**(4), 7–17 (2013)

Bag, R., Mondal, I., Dehbozorgi, M., Bank, S. P., Das, D. N., Bandyopadhyay, J., Pham, Q. B., Al-Quraishi, A. M. F., Nguyen, X. C.: Modelling and mapping of soil erosion susceptibility using machine learning in a tropical hot sub-humid environment. J. Clean. Prod. **364**(2022). https://doi.org/10.1016/j.jclepro.2022.132428

Belasri, A., Lakhouili, A.: Estimation of soil erosion risk using the universal soil loss equation (USLE) and geo-information technology in oued el makhazine watershed, Morocco. J. Geogr. Inform. Syst. **08**(01), 98–107 (2016). https://doi.org/10.4236/jgis.2016.81010

Benavidez, R., Jackson, B., Maxwell, D., Norton, K.: A review of the (revised) universal soil loss equation ((r)usle): with a view to increasing its global applicability and improving soil loss estimates. Hydrol. Earth Syst. Sci. **22**(11), 6059–6086 (2018). https://doi.org/10.5194/hess-22-6059-2018

Beskow, S., Mello, C.R., Norton, L.D., Curi, N., Viola, M.R., Avanzi, J.C.: Soil erosion prediction in the grande river basin, brazil using distributed modeling. Catena **79**(1), 49–59 (2009). https://doi.org/10.1016/j.catena.2009.05.010

Bhat, S.A., Hamid, I., Dar, M.U.D., Rasool, D., Pandit, B.A., Khan, S.: Soil erosion modeling using RUSLE & GIS on micro watershed of J&K. J. Pharmacogn. Phytochem. **6**(5), 838–842 (2017)

Bhatta, B.: Remote Sensing and GIS. Oxford University Press, Oxford (2020)

Bhattacharya, R.K., das Chatterjee, N., Das, K.: Land use and land cover change and its resultant erosion susceptible level: an appraisal using RUSLE and logistic regression in a tropical plateau basin of West Bengal, India. Environ. Dev. Sustain. **23**(2), 1411–1446 (2021). https://doi.org/10.1007/s10668-020-00628-x

Biswas, S.: Estimation of soil erosion using remote sensing and gis and prioritization of catchments. Int. J. Emerg. Technol. Adv. Eng. **2**(7), 124–128 (2012)

Biswas, S.S., Pani, P.: Estimation of soil erosion using RUSLE and GIS techniques: a case study of barakar river basin, Jharkhand, India. Model. Earth Syst. Environ. (2015). https://doi.org/10.1007/s40808-015-0040-3

Chakrabortty, R., Pradhan, B., Mondal, P., Pal, S.C.: The use of RUSLE and GCMs to predict potential soil erosion associated with climate change in a monsoon-dominated region of Eastern India. Arab. J. Geosci. (2020). https://doi.org/10.1007/s12517-020-06033-y

Das, B., Paul, A., Bordoloi, R., Tripathi, O.P., Pandey, P.K.: Soil erosion risk assessment of hilly terrain through integrated approach of RUSLE and geospatial technology: a case study of Tirap district, Arunachal Pradesh. Model. Earth Syst. Environ. **4**(1), 373–381 (2018). https://doi.org/10.1007/s40808-018-0435-z

Das, B., Bordoloi, R., Thungon, L.T., Paul, A., Pandey, P.K., Mishra, M., Tripathi, O.P.: An integrated approach of GIS, RUSLE and AHP to model soil erosion in West Kameng watershed, Arunachal Pradesh. J. Earth Syst. Sci. (2020). https://doi.org/10.1007/s12040-020-1356-6

Demirci, A., Karaburun, A.: Estimation of soil erosion using RUSLE in a GIS framework: a case study in the buyukcekmece lake watershed, northwest Turkey. Environ. Earth Sci. **66**(3), 903–913 (2012). https://doi.org/10.1007/s12665-011-1300-9

Dev Acharya, T., Yang, I.: Exploring landsat 8. International Journal of IT, Engineering and Applied Sciences Research (IJIEASR), **4**(4) (2015)

District survey report of Jalpaiguri district, government of West Bengal. (2021)

Durigon, V.L., Carvalho, D.F., Antunes, M.A.H., Oliveira, P.T.S., Fernandes, M.M.: NDVI time series for monitoring RUSLE cover management factor in a tropical watershed. Int. J. Remote Sens. **35**(2), 441–453 (2014). https://doi.org/10.1080/01431161.2013.871081

FAO-unesco soil map of the world, Paris. (1974)

Ganasri, B.P., Ramesh, H.: Assessment of soil erosion by RUSLE model using remote sensing and GIS—a case study of nethravathi basin. Geosci. Front. **7**(6), 953–961 (2016). https://doi.org/10.1016/j.gsf.2015.10.007

Gayen, A., Saha, S., Pourghasemi, H.R.: Soil erosion assessment using RUSLE model and its validation by FR probability model. Geocarto Int. (2019). https://doi.org/10.1080/10106049.2019.1581272

Ghosh, P., Lepcha, K.: Weighted linear combination method versus grid based overlay operation method—a study for potential soil erosion susceptibility analysis of Malda district (West Bengal) in India. Egypt. J. Remote Sens. Space Sci. **22**(1), 95–115 (2019). https://doi.org/10.1016/j.ejrs.2018.07.002

Ghosh, A., Maiti, R.: Soil erosion susceptibility assessment using logistic regression, decision tree and random forest: study on the mayurakshi river basin of Eastern India. Environ. Earth Sci. (2021). https://doi.org/10.1007/s12665-021-09631-5

Jain, S.K., Kumar, S., Varghese, J.: Estimation of soil erosion for a himalayan watershed using GIS technique. Water Resour. Manag. (2001). https://doi.org/10.1023/A:1012246029263

Knight, E.J., Kvaran, G.: Landsat-8 operational land imager design, characterization and performance. Remote Sens. **6**(11), 10286–10305 (2014). https://doi.org/10.3390/rs61110286

Koirala, P., Thakuri, S., Joshi, S., Chauhan, R.: Estimation of soil erosion in nepal using a RUSLE modeling and geospatial tool. Geosciences (Switzerland) (2019). https://doi.org/10.3390/geosciences9040147

Kulimushi, L.C., Choudhari, P., Mubalama, L.K., Banswe, G.T.: GIS and remote sensing-based assessment of soil erosion risk using RUSLE model in South-Kivu province, eastern, democratic Republic of Congo. Geomatics Nat. Hazards Risk **12**(1), 961–987 (2021). https://doi.org/10.1080/19475705.2021.1906759

Linberger, P.: Center for international earth science information network (CIESIN)—socioeconomic data and applications center (SEDAC). J. Bus. Finance Librariansh. **5**(2), 69–73 (1999). https://doi.org/10.1300/J109v05n02_09

Mahala, A.: Soil erosion estimation using RUSLE and GIS techniques—a study of a plateau fringe region of tropical environment. Arab. J. Geosci. (2018). https://doi.org/10.1007/s12517-018-3703-3

Markose, V.J., Jayappa, K.S.: Soil loss estimation and prioritization of sub-watersheds of Kali river basin, Karnataka, India, using RUSLE and GIS. Environ. Monit. Assess. (2016). https://doi.org/10.1007/s10661-016-5218-2

Mihi, A., Benarfa, N., Arar, A.: Assessing and mapping water erosion-prone areas in northeastern Algeria using analytic hierarchy process, USLE/RUSLE equation, GIS, and remote sensing. Appl. Geomatics. **12**(2), 179–191 (2020). https://doi.org/10.1007/s12518-019-00289-0

Mitra, A.K., Momin, I.M., Rajagopal, E.N., Basu, S., Rajeevan, M.N., Krishnamurti, T.N.: Gridded daily indian monsoon rainfall for 14 seasons: merged TRMM and IMD gauge analyzed values. J. Earth Syst. Sci. **122**(5), 1173–1182 (2013)

Mohammadi, S., Karimzadeh, H., Habashi, K.: Assessment soil erosion and deposition in the menderjan watershed using USPED and RUSLE models in the environment of geographical information system (GIS). Desert Ecosyst. Eng. J. **6**(17), 43–56 (2018)

Moore, I.D., Burch, G.J.: Physical basis of the length-slope factor in the universal Soil loss equation. Soil Sci. Soc. Am. J. **50**, 1294–1298 (1986)

Naqvi, H.R., Mallick, J., Devi, L.M., Siddiqui, M.A.: Multi-temporal annual soil loss risk mapping employing revised universal soil loss equation (RUSLE) model in Nun Nadi Watershed, Uttrakhand (India). Arab. J. Geosci. **6**(10), 4045–4056 (2013). https://doi.org/10.1007/s12517-012-0661-z

Nasir, N., Selvakumar, R.: Influence of land use changes on spatial erosion pattern, a time series analysis using RUSLE and GIS: The cases of Ambuliyar sub-basin, India. Acta Geophys. **66**(5), 1121–1130 (2018). https://doi.org/10.1007/s11600-018-0186-2

Negese, A., Fekadu, E., Getnet, H.: Potential soil loss estimation and erosion-prone area prioritization using RUSLE, GIS, and remote sensing in chereti watershed, Northeastern Ethiopia. Air Soil Water Res. (2021). https://doi.org/10.1177/1178622120985814

Pal, S.C., Shit, M.: Application of RUSLE model for soil loss estimation of Jaipanda watershed, West Bengal. Spat. Inform. Res. **25**(3), 399–409 (2017). https://doi.org/10.1007/s41324-017-0107-5

Pan, J., Wen, Y.: Estimation of soil erosion using RUSLE in Caijiamiao watershed, China. Nat. Hazards. **71**(3), 2187–2205 (2014). https://doi.org/10.1007/s11069-013-1006-2

Pandey, A., Chowdary, V.M., Mal, B.C.: Identification of critical erosion prone areas in the small agricultural watershed using USLE, GIS and remote sensing. Water Resour. Manage. **21**(4), 729–746 (2007). https://doi.org/10.1007/s11269-006-9061-z

Pradeep, G.S., Krishnan, M.V.N., Vijith, H.: Identification of critical soil erosion prone areas and annual average soil loss in an upland agricultural watershed of western ghats, using analytical hierarchy process (AHP) and RUSLE techniques. Arab. J. Geosci. **8**(6), 3697–3711 (2015). https://doi.org/10.1007/s12517-014-1460-5

Prakash, S., Varghese, K.R.B.: Annual soil loss estimation in a Tropical River basin of Southern India using RUSLE model and AHP techniques. J. Geosci. Res. (2022). https://doi.org/10.56153/g19088-021-0068-8

Prasannakumar, V., Shiny, R., Geetha, N., Vijith, H.: Spatial prediction of soil erosion risk by remote sensing, GIS and RUSLE approach: A case study of Siruvani river watershed in Attapady valley, Kerala, India. Environ. Earth Sci. **64**(4), 965–972 (2011). https://doi.org/10.1007/s12665-011-0913-3

Prasannakumar, V., Vijith, H., Abinod, S., Geetha, N.: Estimation of soil erosion risk within a small mountainous sub-watershed in Kerala, India, using revised Universal Soil loss equation (RUSLE) and geo-information technology. Geosci. Front. **3**(2), 209–215 (2012). https://doi.org/10.1016/j.gsf.2011.11.003

Rahaman, S.A., Aruchamy, S., Jegankumar, R., Ajeez, S.A.: EStimation of annual average soil loss, based on rusle model in kallar watershed, Bhavani basin, Tamil NADU, India. Joint international geoinformation conference, 207–214 (2015). https://doi.org/10.5194/isprsannals-II-2-W2-207-2015

Rajbanshi, J., Bhattacharya, S.: Assessment of soil erosion, sediment yield and basin specific controlling factors using RUSLE-SDR and PLSR approach in Konar river basin, India. J. Hydrol. (2020). https://doi.org/10.1016/j.jhydrol.2020.124935

Renard, K.G., Foster, G.R., Weesies, G.A., Porter, J.P.: RUSLE, revised Universal Soil loss equation. J. Soil Water Conserv. **46**(1), 30–33 (1991)

Roy, D., Mitra, R.: Estimation of soil erosion in the Balason river basin using RUSLE modelling of the Darjeeling Himalayan region, India. Res. Square (2022). https://doi.org/10.21203/rs.3.rs-1766179/v1

Saaty, T.L.: The analytic hierarchy process: planning, priority setting, resource allocation. McGraw hill (1980)

Saha, S.K.: Water and wind induced soil erosion assessment and monitoring using remote sensing and GIS. In: Satellite remote sensing and GIS applications in agricultural meteorology, 315–330 (2003)

Saha, A., Ghosh, P., Mitra, B.: GIS based soil erosion estimation using rusle model: a case study of upper Kangsabati watershed, West Bengal, India. Int. J. Environ. Sci. Nat. Resour. (2018). https://doi.org/10.19080/ijesnr.2018.13.555871

Saha, S., Sarkar, D., Mondal, P.: Assessing and mapping soil erosion risk zone in Ratlam District, central India. Reg. Sustain. **3**(4), 373–390 (2022). https://doi.org/10.1016/j.regsus.2022.11.005

Santra, A., Santra Mitra, S.: Space-Time Drought Dynamics and Soil Erosion in Puruliya District of West Bengal, India: A conceptual design. J. Indian Soc. Remote Sens. **48**(8), 1191–1205 (2020). https://doi.org/10.1007/s12524-020-01147-y

Sarkar, B., Islam, A., Majumder, A.: Seawater intrusion into groundwater and its impact on irrigation and agriculture: evidence from the coastal region of West Bengal, India. Reg. Stud. Mar. Sci. (2021). https://doi.org/10.1016/j.rsma.2021.101751

Shit, P.K., Nandi, A.S., Bhunia, G.S.: Soil erosion risk mapping using RUSLE model on jhargram sub-division at West Bengal in India. Model. Earth Syst. Environ. (2015). https://doi.org/10.1007/s40808-015-0032-3

Singh, G., Babu, R., Narain, P., Bhushan, L.S., Abrol, I.P.: Soil erosion rates of India. J. Soil Water Conserv. **47**(1), 97–99 (1992)

Smith, S.J., Williams, J.R., Menzel, R.G., Coleman, G.A.: Prediction of Sediment Yield Plains Grasslands with the versa1 soil loss equation. J. Range Manag. **37**(4), 295–297 (1984)

Tanyaş, H., Kolat, Ã., Süzen, M.L.: A new approach to estimate cover-management factor of RUSLE and validation of RUSLE model in the watershed of Kartalkaya Dam. J. Hydrol. **528**, 584–598 (2015). https://doi.org/10.1016/j.jhydrol.2015.06.048

Teng, H., Liang, Z., Chen, S., Liu, Y., Viscarra Rossel, R.A., Chappell, A., Yu, W., Shi, Z.: Current and future assessments of soil erosion by water on the Tibetan Plateau based on RUSLE and CMIP5 climate models. Sci. Total Environ. **635**, 673–686 (2018). https://doi.org/10.1016/j.scitotenv.2018.04.146

Thomas, J., Joseph, S., Thrivikramji, K.P.: Assessment of soil erosion in a monsoon-dominated mountain river basin in India using RUSLE-SDR and AHP. Hydrol. Sci. J. **63**(4), 542–560 (2018). https://doi.org/10.1080/02626667.2018.1429614

Tirkey, A.S., Pandey, A.C., Nathawat, M.S.: Use of satellite data, GIS and RUSLE for estimation of average annual soil loss in daltonganj watershed of Jharkhand (India). J. Remote Sens. Technol. (2013). https://doi.org/10.18005/jrst0101004

Wawer, R., Nowocieñ, E., Podolski, B.: Real and calculated K_{USLE} erodibility factor for selected polish soils. Polish J. Environ. Stud. **14** (5), 655–658 (2005)

Williams, J.R.: The EPIC model. In: Singh, V.P. (ed.) Computer models of watershed hydrology, pp. 909–1000. Water Resources Publications, Littleton (1995)

Wischmeier, W.H., Smith, D.D.: Rainfall erosion losses from cropland east of the rocky mountains: guide for selection of practices for soil and water conservation, USDA, Washington D.C (Agricultural Handbook No. 282). (1965)

Wischmeier, W.H., Smith, D.D.: Predicting rainfall erosion losses: a guide to conservation planning, USDA, Washington D.C (Agricultural handbook No. 537). (1978)

Yadav, U., Bhardwaj, A.: Accuracy assessment of openly accessible CartoDEM V3 R1 and TanDEM-X 90 using a smartphone with assisted gps for ratlam city and surroundings. 8th Int. Electron. Conf. Sens. Appl. (2022). https://doi.org/10.3390/ecsa-8-11328